

1 ANME-2d anaerobic methanotrophic archaea differ from other ANME
2 archaea in lipid composition and carbon source

3
4 Julia M. Kurth^{ac}, Nadine T. Smit^{bc}, Stefanie Berger^a, Stefan Schouten^{bc}, Mike S.M. Jetten^{acd}, Cornelia
5 U. Welte^{acd}

6 ^a Department of Microbiology, Institute for Water and Wetland Research, Radboud University,
7 Heyendaalseweg 135, 6525 AJ Nijmegen, The Netherlands

8 ^b NIOZ Royal Netherlands Institute for Sea Research, Department of Marine Organic
9 Biogeochemistry and Utrecht University, P.O. Box 59, 1790 AB Den Burg (Texel), The Netherlands

10 ^c Netherlands Earth System Science Center, Utrecht University, Heidelberglaan 2, 3584 CS Utrecht,
11 The Netherlands

12 ^d Soehngen Institute of Anaerobic Microbiology, Radboud University, Heyendaalseweg 135, 6525
13 AJ Nijmegen, The Netherlands

14
15 Correspondence:

16 Julia Kurth, Department of Microbiology, Institute for Water and Wetland Research, Radboud
17 University, Heyendaalseweg 135, 6525 AJ Nijmegen, The Netherlands; j.kurth@science.ru.nl.

18 Cornelia Welte, c.welte@science.ru.nl.

19

20 Abstract

21 The anaerobic oxidation of methane (AOM) is a microbial process present in marine and freshwater
22 environments. AOM is important for reducing the emission of the second most important greenhouse
23 gas methane. In marine environments anaerobic methanotrophic archaea (ANME) are involved in
24 sulfate-reducing AOM. In contrast, *Ca. Methanoperedens* of the ANME-2d cluster carries out nitrate
25 AOM in freshwater ecosystems. Despite the importance of those organisms for AOM in non-marine
26 environments not much is known about their lipid composition or carbon sources. To close this gap,
27 we analyzed the lipid composition of ANME-2d archaea and found that they mainly synthesize
28 archaeol and hydroxyarchaeol as well as different (hydroxy-) glycerol dialkyl glycerol tetraethers,
29 albeit in much lower amounts. Abundant lipid headgroups were dihexose, monomethyl-phosphatidyl
30 ethanolamine and phosphatidyl hexose. Moreover, a monopentose was detected as a lipid headgroup
31 which is rare among microorganisms. Batch incubations with ^{13}C labelled bicarbonate and methane
32 showed that methane is the main carbon source of ANME-2d archaea varying from ANME-1 archaea
33 which primarily assimilate dissolved inorganic carbon (DIC). ANME-2d archaea also assimilate DIC,
34 but to a lower extent than methane. The lipid characterization and analysis of the carbon source of *Ca.*
35 *Methanoperedens* facilitates distinction between ANME-2d and other ANMEs.

36 Introduction

37 Methane is the second most important greenhouse gas on earth with an atmospheric methane budget of
38 about 600 Tg per year (Conrad, 2009; Dean *et al.*, 2018). About 69% of methane emission into the
39 atmosphere is caused by methanogenic archaea (Conrad, 2009). Fortunately aerobic and anaerobic
40 methanotrophic microorganisms can oxidize methane back to carbon dioxide that is a 25-times less
41 potent greenhouse gas than methane. The anaerobic oxidation of methane (AOM) is a microbial
42 process present in marine and freshwater environments. AOM has first been described to be performed
43 by a consortium of anaerobic methanotrophic archaea (ANME) and sulfate-reducing bacteria in
44 microbial mats in the deep sea or in marine sediments (Hoehler *et al.*, 1994; Hinrichs *et al.*, 1999;
45 Boetius *et al.*, 2000; Hinrichs and Boetius, 2002; Orphan *et al.*, 2002). ANME archaea are related to
46 methanogens and oxidize methane by using the reverse methanogenesis pathway (Hallam *et al.*, 2004;
47 Arshad *et al.*, 2015; McAnulty *et al.*, 2017; Timmers *et al.*, 2017). In addition to sulfate, also oxidized
48 nitrogen compounds (Raghoebarsing *et al.*, 2006; Ettwig *et al.*, 2010; Haroon *et al.*, 2013) as well as
49 iron and manganese (Beal *et al.*, 2009; Ettwig *et al.*, 2016; Cai *et al.*, 2018) can be used as electron
50 acceptors within the AOM process.

51 Anaerobic methanotrophic archaea can be assigned to three distinct clusters within the Euryarchaeota,
52 ANME-1, ANME-2 and ANME-3, which are related to the orders *Methanosarcinales* and
53 *Methanomicrobiales* (Knittel and Boetius, 2009). The phylogenetic distance between the groups is
54 quite large (16S rRNA gene sequence identity between 75-92%) (Knittel and Boetius, 2009). Most
55 analysed members of the three ANME clades have been described to perform sulfate driven AOM in
56 marine environments (Pancost *et al.*, 2001; Blumenberg *et al.*, 2004; Niemann and Elvert, 2008;
57 Rossel *et al.*, 2008; Wegener *et al.*, 2008; Kellermann *et al.*, 2012). However, members of the ANME-
58 2d cluster have not been found in consortia with sulfate reducers. Instead, ANME-2d archaea are the
59 main players in nitrate-dependent AOM. Microorganisms conducting nitrate AOM have been enriched
60 from anoxic freshwater sediments, digester sludge and rice paddies (Raghoebarsing *et al.*, 2006; Hu *et al.*,
61 2009; Arshad *et al.*, 2015; Vaksmaa, Guerrero-Cruz, *et al.*, 2017). Denitrifying AOM can either be
62 conducted by a consortium of nitrate-reducing ANMEs, *Ca. Methanoperedens* sp., and nitrite reducing
63 NC10 bacteria, *Ca. Methylomirabilis* sp. (Raghoebarsing *et al.*, 2006; Haroon *et al.*, 2013; Arshad
64 *et al.*, 2015) or by a consortium of those ANME archaea and anammox bacteria (Haroon *et al.*, 2013). In
65 those consortia *Ca. Methylomirabilis* sp. or anammox bacteria are important to reduce the toxic nitrite
66 produced during nitrate AOM by *Ca. Methanoperedens* sp.

67 To understand the prevalence of anaerobic methane oxidation in past and present environments and
68 identify the key players at different environmental sites, it is necessary to identify biomarkers for those
69 organisms. As core lipids are much more stable than DNA over time, lipid biomarkers are a useful tool
70 to trace microorganisms and therefore specific microbial processes back in time. Moreover, intact
71 polar lipids are crucial to examine present microbial communities and to distinguish between different
72 microorganisms (Ruetters *et al.*, 2002; Sturt *et al.*, 2004). Quite some information is available on core
73 and intact polar lipids as well as on carbon assimilation in marine AOM consortia of ANME archaea
74 and sulfate-reducing bacteria (Pancost *et al.*, 2001; Blumenberg *et al.*, 2004; Niemann and Elvert,
75 2008; Rossel *et al.*, 2008; Wegener *et al.*, 2008; Kellermann *et al.*, 2012). In contrast, lipids from one
76 of the main players in denitrifying AOM, *Ca. Methanoperedens* sp., have hardly been studied: a
77 preliminary study on the lipids of a culture containing *Ca. Methanoperedens* sp. and *Ca.*

78 *Methylophilum oxyfera* only detected sn2-hydroxyarchaeol as the dominant lipid of the archaeal
79 partner (Raghoebarsing *et al.*, 2006).

80 Besides the characterization of lipids in ANME archaea it is also pivotal to understand which carbon
81 source those organisms use for biomass production. The main carbon assimilation pathway in
82 methanogenic Euryarchaeota is the reductive acetyl-CoA pathway (Whitman, 1994; Berg *et al.*, 2010).
83 In this pathway a carbonyl group and a methyl group are combined to form acetyl-CoA. In archaea,
84 acetyl-CoA is used for formation of membrane lipids via the isoprenoid compound
85 geranylgeranylphosphate in the mevalonate pathway, although not all of the enzymes involved in this
86 pathway are known with certainty (Koga and Morii, 2007; Matsumi *et al.*, 2011). An ether bond is
87 formed between the glycerol-1-phosphate backbone and the isoprenoid side chains. Subsequently
88 cytidine-diphosphate is attached and finally the unsaturated isoprenoid side chains are reduced to form
89 diphytanylglycerol diether, also known as archaeol (Matsumi *et al.*, 2011).

90 The isotopic composition of lipids provides information on the carbon source used by the
91 microorganism. The lipids of ANMEs involved in AOM are usually strongly depleted in ^{13}C , with
92 $\delta^{13}\text{C}$ values ranging from -70 to -130% (Elvert *et al.*, 1999; Pancost *et al.*, 2000; Niemann and Elvert,
93 2008). Such low $\delta^{13}\text{C}$ values of lipids have been explained by the assimilation of ^{13}C -depleted methane
94 carbon during methane uptake into biomass (Elvert *et al.*, 1999; Hinrichs *et al.*, 1999; Pancost *et al.*,
95 2000; Orphan *et al.*, 2002). Mixed assimilation of CH_4 and CO_2 has been reported for marine ANME-
96 1, -2a, and -2b strains indicating that at least some ANME strains can use methane-derived carbon for
97 biomass production (Wegener *et al.*, 2008). However, for ANME-1 it has been shown that methane
98 oxidation is decoupled from the assimilatory system and that CO_2 -dependent autotrophy is the
99 predominant mode of carbon fixation (Kellermann *et al.*, 2012). In general, ANME archaea seem to be
100 able to assimilate both, methane and dissolved inorganic carbon, and the preferred carbon source for
101 assimilation might vary between the different ANME clusters.

102 In this study, we performed analysis of the lipids from ANME-2d archaea and compared these with
103 previous studies about different ANME lipids. Moreover, we analysed the incorporation of ^{13}C -
104 labelled methane and bicarbonate in lipids of these archaea to establish the carbon sources used for
105 assimilation.

106 **Methods**

107 **ANME-2d bioreactor operation and sampling for lipid analysis**

108 For lipid analysis of *Ca. Methanoperedens* sp. two different bioreactors were sampled. One bioreactor
109 contained archaea belonging to the ANME-2d clade enriched from the Ooijpolder (NL) (Arshad *et al.*,
110 2015; Berger *et al.*, 2017) and the other reactor ANME-2d archaea enriched from an Italian paddy
111 field (Vaksmas, Jetten, *et al.*, 2017). The anaerobic enrichment culture dominated by *Ca.*
112 *Methanoperedens* sp. strain BLZ2 originating from the Ooijpolder (Berger *et al.*, 2017) was
113 maintained in an anaerobic 10 L sequencing batch reactor (30°C, pH 7.3 ± 0.1, stirred at 180 rpm).
114 The mineral medium consisted of 0.16 g/L MgSO₄, 0.24 g/L CaCl₂ and 0.5 g/L KH₂PO₄. Trace
115 elements and vitamins were supplied using stock solutions. 1000 x trace element stock solution: 1.35
116 g/L FeCl₂ x 4 H₂O, 0.1 g/L MnCl₂ x 4 H₂O, 0.024 g/L CoCl₂ x 6 H₂O, 0.1 g/L CaCl₂ x 2 H₂O, 0.1 g/L
117 ZnCl₂, 0.025 g/L CuCl₂ x 2 H₂O, 0.01 g/L H₃BO₃, 0.024 g/L Na₂MoO₄ x 2 H₂O, 0.22 g/L NiCl₂ x 6
118 H₂O, 0.017 g/L Na₂SeO₃, 0.004 g/L Na₂WO₄ x 2 H₂O, 12.8 g/L nitrilotriacetic acid; 1000 x vitamin
119 stock solution: 20 mg/L biotin, 20 mg/L folic acid, 100 mg/L pyridoxine-HCl, 50 mg/L thiamin-HCl x
120 2 H₂O, 50 mg/L riboflavin, 50 mg/L nicotinic acid, 50 mg/L D-Ca-pantothenate, 2 mg/L vitamin B12,
121 50 mg/L p-aminobenzoic acid, 50 mg/L lipoic acid. The medium supply was continuously sparged
122 with Ar:CO₂ in a 95:5 ratio. Per day 30 mmol nitrate added to the medium were supplied to the
123 bioreactor and were completely consumed. Methane was added by continuously sparging the reactor
124 content with CH₄:CO₂ in a 95:5 ratio at a rate of 15 mL/min. The reactor was run with a medium
125 turnover of 1.25 L per 12 h. A 5 min settling phase for retention of biomass preceded the removal of
126 supernatant. Under these conditions nitrite was not detectable with a colorimetric test with a lower
127 detection limit of 2 mg/L (MQuant test stripes, Merck, Darmstadt, Germany). Growth conditions and
128 operation of the bioreactor containing ANME-2d archaea enriched from an Italian paddy field soil are
129 described by Vaksmas *et al.*, 2017 (Vaksmas, Jetten, *et al.*, 2017). Sampled material from both reactors
130 was centrifuged (10000 x g, 20 min, 4°C) and pellets were kept at -80°C until subsequent freeze-
131 drying and following lipid and isotope analysis.

132

133 **Analysis of the microbial community**

134 For the Ooijpolder enrichment we performed whole genome metagenome sequencing. DNA
135 extraction, library preparation and metagenome sequencing were performed as described before by
136 Berger and co-workers (Berger *et al.*, 2017). Quality-trimming, sequencing adapter removal and
137 contaminant filtering of Illumina paired-end sequencing reads were performed using BBTools BBDuk
138 37.76 (BBMap - Bushnell B. - sourceforge.net/projects/bbmap/). Processed paired-end reads were
139 assigned to a taxon using Kaiju 1.6.2 (Menzel *et al.*, 2016) employing the NCBI BLAST non-
140 redundant protein database (NCBI Resource Coordinators, 2016).

141

142 **Batch cultivation of ANME-2d bioreactor cell material for ¹³C-labelling experiment**

143 60 ml bioreactor material of a *Ca. Methanoperedens* sp. BLZ2 culture enriched from the Ooijpolder
144 (Arshad *et al.*, 2015; Berger *et al.*, 2017) were transferred with a syringe to a 120-ml serum bottle that
145 had been made anoxic by flushing the closed bottle with argon gas for 10 min. Afterwards, the culture
146 was purged with 90% argon and 10% CO₂ for 5 min. 2.5 mM NaHCO₃ and 18 ml methane (Air

147 Liquide, Eindhoven, The Netherlands) were added. Except for the negative controls, either ¹³C-
148 labelled methane (99 atom%; Isotec Inc., Matheson Trigas Products Division) or ¹³C-labelled
149 bicarbonate (Cambridge Isotope Laboratories Inc., Tewksbury, USA) was used in the batch
150 incubations. The bottles were incubated horizontally on a shaker at 30°C and 250 rpm for one or three
151 days. All bottles contained sodium nitrate (0.6 mM) at the start of incubation and additional nitrate
152 was added when the concentration in the bottles was close to 0, as estimated by MQuant (Merck,
153 Darmstadt, Germany) test strips. The methane concentration in the headspace was measured twice a
154 day by gas chromatography with a gas chromatograph (Hewlett Packard 5890a, Agilent Technologies,
155 Santa Clara CA, US) equipped with a Poropak Q 100/120 mesh and a thermal conductivity detector
156 (TCD) using N₂ as carrier gas. Each measurement was performed by injection of 50 µl headspace gas
157 with a gas-tight syringe. With this technique a decrease in methane concentration from ~24 % to ~20
158 % within three days of incubation was observed. After batch incubation, cell material was centrifuged
159 (10000 x g, 20 min, 4°C) and pellets were kept at -80°C until subsequent freeze-drying and following
160 lipid and isotope analysis. It has to be considered that cultures with ¹³C-labelled bicarbonate also
161 contained ¹²C derived from CO₂. Having in mind that 10% of CO₂ were added to the culture (pCO₂=
162 0.1 atm) the CO₂ concentration in the solution was calculated to be about 3.36 mM by use of the
163 equation [CO₂]_{aq}= pCO₂/k_h (Henry constant (k_h) is 29.76 atm/(mol/L) at 25°C). Therefore, it has to be
164 assumed that about half of the carbon in the cultures where ¹³C labelled bicarbonate was added derived
165 from ¹²C-CO₂ dissolved in the medium after gassing with a mixture of 10% CO₂/90% Ar gas.

166

167 **Lipid extraction and analysis**

168 **Bligh and Dyer extraction** - Lipids of freeze-dried biomass (between 20 and 70 mg) were extracted by
169 a modified Bligh and Dyer method as described by Bale et al. (Bale *et al.*, 2013) using a mixture of
170 methanol, dichloromethane and phosphate buffer at pH 7.4 (2:1:0.8 v/v/v). After ultrasonic extraction
171 (10 min) and centrifugation the solvent layer was collected. The residue was re-extracted twice. The
172 combined solvent layers were separated by adding additional DCM and phosphate buffer to achieve a
173 ratio of MeOH, DCM and phosphate buffer (1:1:0.9 v/v/v). The separated organic DCM layer on the
174 bottom was removed and collected while the aqueous layer was washed two more times with DCM.
175 The combined DCM layer was evaporated under a continuous stream of nitrogen.

176 **Acid hydrolysis** - Head groups of archaeal lipids were removed using acid hydrolysis. About 20 mg
177 freeze-dried biomass was hydrolyzed with 2 ml of a 1.5 N HCl/MeOH solution and samples stirred for
178 2 h while heated at 130°C with a reflux system. After cooling, the pH was adjusted to pH 4-5 by
179 adding 2 N KOH/MeOH solution. 2 ml DCM and 2 ml distilled H₂O were added. The DCM bottom
180 layer was transferred to a new vial and the MeOH/H₂O layer washed twice with DCM. Combined
181 DCM layers were dried over a Na₂SO₄ column and the solvent removed by evaporation under a stream
182 of nitrogen.

183 **BF₃ methylation and silylation** - For gas chromatography (GC) analysis aliquots of the acid
184 hydrolyzed samples were methylated using 0.5 ml of BF₃-methanol and react for 10 min at 60°C in a
185 oven. 0.5 ml H₂O and 0.5 ml DCM were added to the heated mixture to separate the DCM and
186 aqueous layers. Samples were mixed, centrifuged and the DCM-layer taken off and collected. The
187 water layer was washed three more times with DCM. The combined DCM-layer were evaporated
188 under a N₂ stream and water was removed by use of a MgSO₄ column. After dissolving the sample in

189 ethyl acetate, the extract was cleaned over a small silicagel column and lipids were eluted with ethyl
190 acetate. The extract was dried under N₂. For GC analysis, extracts (0.3 to 0.5 mg) were dissolved in 10
191 µl pyridine and 10 µl BSTFA. Samples were heated for 30 min at 60°C and afterwards diluted with
192 ethyl acetate to 1 mg/ml.

193 **GC-MS** – Gas chromatography linked to mass spectrometry (GC-MS) was performed with a 7890B
194 gas chromatography system (Agilent) connected to a 7000 GC/MS Triple Quad (Agilent). The gas
195 chromatograph was equipped with a fused silica capillary column (25 m x 0.32 mm) coated with CP
196 Sil-5 CB (0.12 µm film thickness) and a Flame Ionization Detector (FID). Helium was used as the
197 carrier gas. The samples were injected manually at 70°C via an on-column injector. The oven
198 temperature was programmed to a temperature increase from 70 to 130°C with 20°C/min and a further
199 increase to 320°C with 4°C/min to, 320°C was held for 10 min. The mass range of the mass
200 spectrometer was set to scan from m/z 50 to m/z 850.

201 **GC-IRMS** – Gas chromatography coupled to isotope-ratio mass spectrometry (GC-IRMS) was
202 performed on a TRACE 1310 Gas Chromatograph (Thermo Fisher Scientific) interfaced with a
203 Scientific GC IsoLink II Conversion Unit connected to an IRMS DELTA V Advantage Isotope-ratio
204 mass spectrometer (Thermo Fisher Scientific). The gas chromatograph was equipped with a fused
205 silica capillary column (25 m x 0.32 mm) coated with CP Sil-5 CB (0.12 µm film thickness). Helium
206 was used as the carrier gas. The samples were injected at 70°C via an on-column injector. The oven
207 temperature was programmed to a temperature increase from 70 to 130°C with 20°C/min and a further
208 increase to 320°C with 4°C/min, 320°C was held for 10 min. δ¹³C values were corrected for methyl
209 group derived from BF₃ methanol in case of carboxylic acid group (bacterial lipids) and methyl groups
210 derived from BSTFA in case of hydroxyl groups (mainly archaeal lipids). Averaged δ¹³C values are
211 based on experimental triplicates, but not on analytical duplicates.

212 **UHPLC-APCI-TOF-MS** - About 0.4 to 0.8 mg of the acid hydrolyzed lipid extract was dissolved in a
213 mixture of hexane/isopropanol 99:1. Extracts were filtered by use of a 0.45 µm, 4 mm diameter PTFE
214 filter. About 2 mg per ml core lipid containing extracts were used for analysis by ultra-high
215 performance liquid chromatography linked to time-of-flight atmospheric pressure chemical ionization
216 mass spectrometry using a (UHPLC-APCI-TOFMS). Core lipid analysis was performed on an Agilent
217 1260 Infinity II UHPLC coupled to an Agilent 6230 TOF-MS. Separation was achieved on two
218 UHPLC silica columns (BEH HILIC columns, 2.1 x 150 mm, 1.7 µm; Waters) in series maintained at
219 25°C. The injection volume was 10 µl. Lipids were eluted isocratically for 10 min with 10% B,
220 followed by a linear gradient to 18% B in 15 min, then a linear gradient to 30% B in 25 min, then a
221 linear gradient to 100% B in 30 min, and finally 100% B for 20 min, where A is hexane and B is
222 hexane: isopropanol (9:1). Flow rate was 0.2 ml/min and pressure 400 bar. Total run time was 120 min
223 with a 20 min re-equilibration. Settings of the ion source (APCI) were as followed: gas temperature
224 200°C, vaporizer 400°C, drying gas 6 l/min, nebulizer 60 psig. The lipids were identified using a
225 positive ion mode (600–1400 m/z). 4mm PTFE filter (polypropylene...).

226 **UHPLC-ESI-MS** - 0.3 to 0.7 mg of Bligh and Dyer sample was dissolved in an injection solvent
227 composed of hexane/isopropanol/water (72:27:1;v/v/v) and filtered through a 0.45 µm regenerated
228 cellulose filter with 4 mm diameter prior to analysis by ultra-high performance liquid chromatography
229 linked to ion trap mass spectrometry using electrospray ionization (UHPLC-ESI-MS). UHPLC
230 separation was conducted on an Agilent 1200 series UHPLC equipped with a YMC-Pack Diol-120-NP

231 column (250 x 2.1 mm, 5 μ m particle size) and a thermostated autoinjector, coupled to a Thermo LTQ
232 XL linear ion trap with Ion Max source with electrospray ionization (ESI) probe (Thermo Scientific,
233 Waltham, MA). Solvent A contained 79% hexane, 20% isopropanol, 0.12% formic acid, 0.04%
234 ammonium and solvent B 88% isopropanol, 10 % H₂O, 0.12% formic acid, 0.04% ammonium. Lipids
235 were eluted with 0% B for 1 min, a linear gradient from 0 to 34% B in 17 min, 34% B for 12 min,
236 followed by a linear gradient to 65% B in 15 min, 65% B for 15 min and finally a linear gradient to
237 100% B in 15 min. The IPLs were identified using a positive ion mode (m/z 400–2000) and a collision
238 energy of 35 eV.

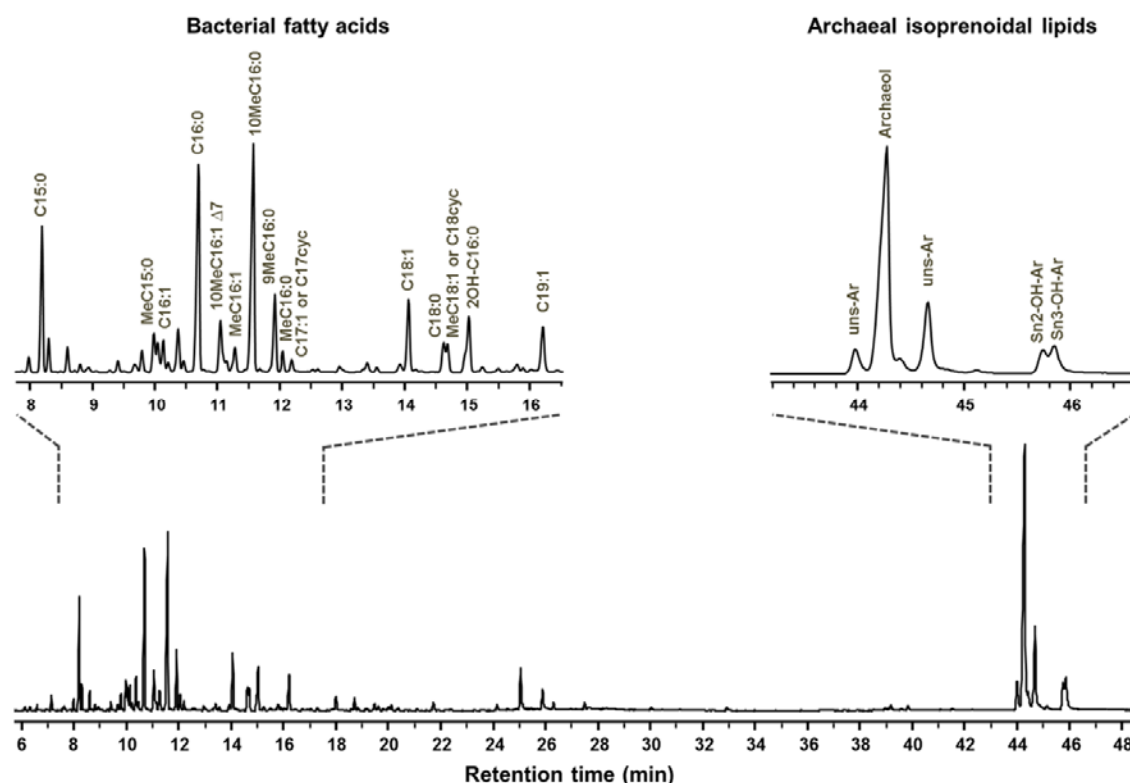
239 Results and Discussion

240 Analysis of microbial community

241 We performed phylogenetic analysis of the microbial community in the ANME-2d enrichment
242 originating from the Ooijpolder. Twenty-three percent of the reads were assigned to *Ca.*
243 *Methanoperedens* sp. strain BLZ2, 33% to *Ca.* *Methylomirabilis* sp. acting as nitrite scavenger, 8% to
244 Alphaproteobacteria, 6% to Gammaproteobacteria, 5% to Betaproteobacteria 1% to
245 Deltaproteobacteria, 3% to Terrabacteria, 3% to Sphingobacteria and 1% to Planctobacteria. The only
246 archaeon in the bioreactor was *Ca.* *Methanoperedens* sp. strain BLZ2. Analysis of the microbial
247 community in the Italian paddy field ANME-2d enrichment has been described by Vaksmaa et al.,
248 2017. For this bioreactor a similar proportion (22%) of ANME-2d archaea, in this case *Ca.*
249 *Methanoperedens* sp. strain Vercelli, was detected. In this study we mainly show the results derived
250 from lipid analysis of the *Ca.* *Methanoperedens* sp. BLZ2 enrichment originating from the Ooijpolder
251 (Arshad *et al.*, 2015; Berger *et al.*, 2017). However, the results deriving from a *Ca.* *Methanoperedens*
252 sp. Vercelli enrichment originating from Italian paddy field soil (Vaksmaa, Jetten, *et al.*, 2017) look
253 very similar, indicating that our results are not dependent on the strain or the environment from which
254 the strain was enriched.

255 Core lipids of *Ca. Methanoperedens* sp.

256 To analyze the lipids of ANME-2d archaea, biomass from a bioreactor containing *Ca.*
257 *Methanoperedens* sp. BLZ2 enrichment was sampled and core lipid analysis with GC-MS and
258 UHPLC-APCI-TOF-MS was performed.



259

260 **Figure 1: Gas chromatogram of core lipids released by acid hydrolysis from *Ca. Methanoperedens* sp.**
261 **(ANME-2d) enrichment.**

262 The enriched biomass of ANME-2d originates from the Ooijpolder (NL) (Arshad *et al.*, 2015). Enlarged inserts
263 show the TIC (total ion chromatogram) of the bacterial and archaeal lipids. The most abundant compounds are
264 annotated with their compound name and following abbreviations: Uns-Ar = monounsaturated archaeol, OH-Ar
265 = hydroxyarchaeol.

266 GC analysis of the core lipids released by acid hydrolysis showed that of the microbial community
267 harbored bacterial fatty acids and isoprenoidal archaeal lipids (Figure 1). We detected the typical
268 membrane lipids of *Ca. Methylomirabilis* sp., namely 10-methylhexadecanoic acid (10MeC_{16:0}) and its
269 monounsaturated variant (10MeC_{16:1Δ7}) (Kool *et al.*, 2012). The archaeal isoprenoids were
270 predominantly composed of archaeol with lower amounts of sn2-hydroxyarchaeol and sn3-
271 hydroxyarchaeol as well as two monounsaturated archaeols (Nichols and Franzmann, 1992).
272 Monounsaturated archaeol has already been described to be present in samples of archaea associated
273 with anaerobic methane oxidation in marine environments (Pancost *et al.*, 2001; Blumenberg *et al.*,
274 2005). However, the monounsaturated archaeol might be produced from hydroxyarchaeol during
275 acidic treatment of the lipids and therefore might not be part of native membrane lipid structures
276 (Ekiel and Sprott, 1992). Alternation of the hydroxyarchaeol structure caused by different reaction
277 conditions during lipid treatment has also been shown by Hinrichs and co-workers (Hinrichs *et al.*,
278 2000). On the other hand, monounsaturated archaeols have also been described for *Halorubrum*
279 *lacusprofundi* (Franzmann *et al.*, 1988; Gibson *et al.*, 2005), *Methanopyrus kandleri* (Nishihara *et al.*,

280 2002), *Methanococcoides burtonii* (Nichols and Franzmann, 1992; Nichols *et al.*, 1993), even if using
 281 mild alkaline hydrolysis instead of acidic treatment for lipid extraction (Nishihara *et al.*, 2002).

282 One possibility to distinguish between the different ANME groups is the sn2-hydroxyarchaeol to
 283 archaeol proportion (Blumenberg *et al.*, 2004). For ANME-1 this ratio is described to be 0-0.8, for
 284 marine ANME-2 1.1 to 5.5 and for ANME-3 within the range of ANME-2 (Blumenberg *et al.*, 2004;
 285 Niemann *et al.*, 2006; Nauhaus *et al.*, 2007; Niemann and Elvert, 2008). In our study with the non-
 286 marine ANME-2d archaea we observed a sn2-hydroxyarchaeol to archaeol ratio of around 0.2. As
 287 mentioned before, the monounsaturated archaeol species might be an artefact of hydroxyarchaeol. If
 288 the monounsaturated archaeols are added to that of the sn2-hydroxyarchaeol abundance, the ratio
 289 would still be only around 0.3. That means that the hydroxyarchaeol to archaeol ratio of ANME-2d is
 290 more similar to that of ANME-1 archaea than to that of other ANME-2 or ANME-3 archaea. Members
 291 of the related methanogen order *Methanomicrobiales* only contain archaeol and GDGT-0 in their
 292 membranes but not hydroxyarchaeol (Koga *et al.*, 1998). In the order *Methanosarcinales* the lipid
 293 composition varies between the different members. Most strains produce archaeol and
 294 hydroxyarchaeol, but the ratio differs and also the type of hydroxyarchaeol isomer varies.
 295 *Methanosarcinaceae* mainly produce the sn2-isomer, whereas *Methanosaetaceae* mainly produce the
 296 rare sn3-isomer (Koga *et al.*, 1998).

297 Subsequently, UHPLC-APCI-TOF-MS analysis of the lipid extract was conducted in order to obtain
 298 information about the tetraether lipids. This revealed that the relative abundance of archaeol was two
 299 times higher than that of glycerol dialkyl glycerol tetraethers (GDGTs) (Table 1). Moreover, several
 300 types of GDGTs were present in the enrichment. GDGTs contained either no (GDGT-0), one (GDGT-
 301 1) or two (GDGT-2) cyclopentane rings and about 64% of the GDGTs were hydroxylated (OH-
 302 GDGTs). The most abundant GDGTs were GDGT-0 with 6% and di-OH-GDGT-2 with 5% of total
 303 lipids. In conclusion, ANME-2d archaea synthesize various core-GDGTs, however archaeol and its
 304 homologues are the main isoprenoidal core-lipids in this enrichment.

305 **Table 1: Abundance of archaeol and GDGTs of *Ca. Methanoperedens* sp.**

306 Lipid extraction was performed in quadruplicates, error is given as standard deviation. For calculation of the
 307 relative abundance of archaeol also peaks derived from archaeol artefacts created during the experimental
 308 procedure were used.

Lipid	Relative abundance (%)	Relative abundance (%)
Archaeol	68 ± 5	68 ± 5
GDGT-0	6 ± 1	
GDGT-1	3 ± 1	
GDGT-2	2 ± 1	
OH-GDGT-1	3 ± 1	
OH-GDGT-2	1 ± 1	32 ± 5
di-OH-GDGT-1	3 ± 2	
di-OH-GDGT-2	5 ± 2	
other GDGT-2 derivatives	9 ± 4	

309 Environmental samples from Mediterranean cold seeps with marine AOM associated archaea mainly
 310 contained GDGTs with 0 to 2 cyclopentane rings (Pancost *et al.*, 2001). In a study on distinct
 311

312 compartments of AOM-driven carbonate reefs growing in the northwestern Black Sea, GDGTs could
313 only be found in samples when ANME-1 archaea were present, but not when only ANME-2 archaea
314 were found, which led to the conclusion that ANME-2 archaea are not capable of synthesizing
315 internally cyclized GDGT (Blumenberg *et al.*, 2004). Later on in a study on methanotrophic consortia
316 at cold methane seeps, samples associated with ANME-2c were shown to contain relatively high
317 amounts of GDGTs (Elvert *et al.*, 2005). In general, GDGTs are dominant in ANME-1 communities,
318 while in marine ANME-2 and ANME-3 communities archaeol derivatives are most abundant
319 (Niemann and Elvert, 2008; Rossel *et al.*, 2008). Members of the related methanogen order
320 *Methanomicrobiales* produce relatively high amounts of GDGT-0 (Koga *et al.*, 1998; Schouten *et al.*,
321 2012), whereas *Methanosarcinales* produce no or only minor amounts of GDGTs, mainly GDGT-0
322 (De Rosa and Gambacorta, 1988; Nichols and Franzmann, 1992; Schouten *et al.*, 2012). Hydroxylated
323 GDGTs seem to be relatively rare. In marine sediment samples the hydroxy-GDGT to total core
324 GDGT ratio has been shown to vary between 1 and 8 % and the dihydroxy-GDGT to total core GDGT
325 ratio is below 2% (Liu *et al.*, 2012). Hydroxylated GDGTs have so far only been identified in the
326 methanogenic Euryarchaeon *Methanothermococcus thermolithotrophicus* (Liu *et al.*, 2012) and in
327 several Thaumarchaeota (Schouten *et al.*, 2012; Sinninghe Damsté *et al.*, 2012). Until now only
328 hydroxylated GDGTs with 0 to 2 cyclopentane rings have been found (Liu *et al.*, 2012; Schouten *et al.*,
329 *et al.*, 2012; Sinninghe Damsté *et al.*, 2012).

330

331 Comparing the results obtained in this study and lipid characterizations of marine ANMEs, it is
332 apparent that the ratio of archaeol and GDGTs are distinctive in the different ANME groups: ANME-1
333 and partially ANME-2c contain substantial amounts of GDGTs and especially in ANME-1, GDGTs
334 are the predominant membrane lipids (Niemann and Elvert, 2008). In contrast to ANME-1, but similar
335 to other ANME-2 and ANME-3, we found that the dominating lipids in the membrane of clade
336 ANME-2d archaea were archaeol variants and not GDGTs. However, about 30% of the membrane
337 lipids in ANME-2d archaea were GDGTs. Most strikingly, the majority of those GDGTs were
338 hydroxylated, which is quite rare and has not been observed for other ANMEs so far.

339

340 **Intact polar lipids of *Ca. Methanoperedens* sp.**

341 Although intact polar lipids (IPLs) degrade more quickly than core lipids, IPLs are of higher
342 taxonomic specificity and therefore useful to study especially present environments (Ruetters *et al.*,
343 2002; Sturt *et al.*, 2004). To identify IPLs of *Ca. Methanoperedens* archaea, UHPLC-ESI-MS was
344 performed.

345 The three most abundant archaeal IPLs detected were archaeol with a dihexose headgroup and
346 hydroxyarchaeol with either a monomethyl phosphatidyl ethanolamine (MMPE) or a phosphatidyl
347 hexose (PH) headgroup. Further headgroups attached to archaeol were monohexose, MMPE, dimethyl
348 phosphatidyl ethanolamine (DMPE), phosphatidyl ethanolamine (PE) and PH. Next to MMPE and
349 PH, hydroxyarchaeol based IPLs also contained dihexose, monopentose, DMPE, PE, pentose-MMPE,
350 hexose-MMPE and pentose-PE. Headgroups of GDGTs were found to be diphosphatidyl glycerol and
351 dihexose phosphatidyl glycerol. The identification of a pentose as a headgroup of hydroxyarchaeol
352 (mass loss of m/z 132) was unexpected. To our knowledge, this is the first description of a pentose as
353 headgroup for microbial IPLs.

354 ANME-1 archaea mainly produce diglycosidic GDGTs, whereas lipids of marine ANME-2 and
355 ANME-3 are dominated by phosphate-based polar derivatives of archaeol and hydroxyarchaeol
356 (ANME-2: phosphatidyl glycerol, phosphatidyl ethanolamine, phosphatidyl inositol, phosphatidyl
357 serine, dihexose; ANME-3: phosphatidyl glycerol, phosphatidyl inositol, phosphatidyl serine) (Rossel
358 *et al.*, 2008). Furthermore, marine ANME-2 archaea produce only minor amounts of GDGT-based
359 IPLs and ANME-3 archaea produce no GDGT-based IPLs at all (Rossel *et al.*, 2008). IPLs of ANME-
360 2d archaea can be distinguished from those of ANME-1 archaea by the prevalence of phosphate
361 containing headgroups as well as archaeol and hydroxyarchaeol based IPLs. Furthermore, ANME-2d
362 can be distinguished from other ANME-2 and ANME-3 archaea by the high abundance of dihexose as
363 headgroup, the rare MMPE and DMPE headgroups and putatively also the pentose headgroup, which
364 so far has not been described in the literature. In contrast to ANME-3 archaea, ANME-2d and marine
365 ANME-2 archaea produce GDGT-based IPLs, albeit only in minor amounts.

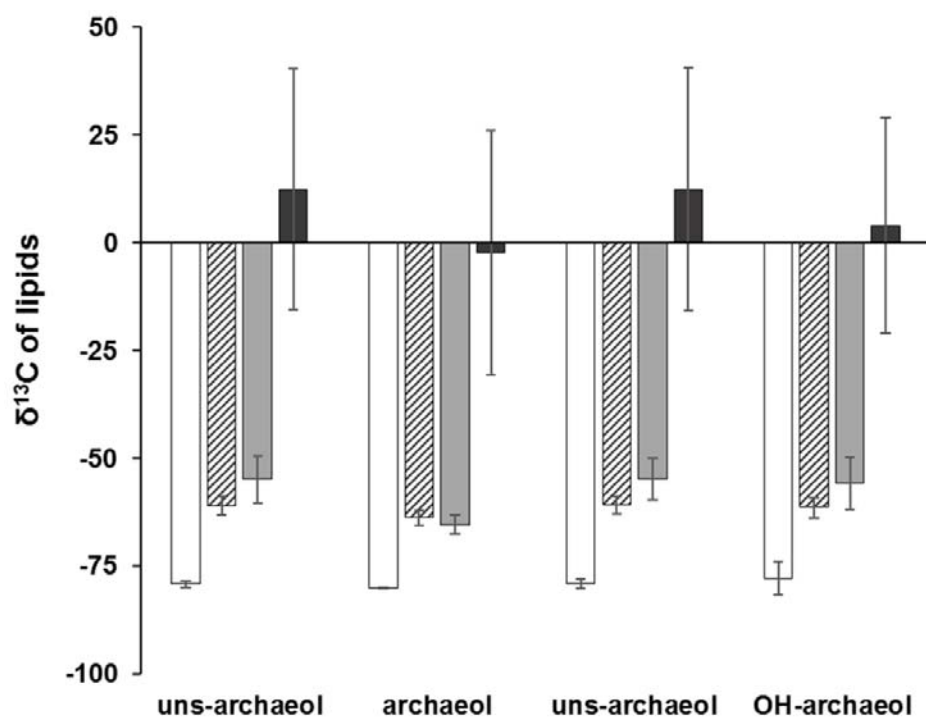
366 In marine environments, a variety of archaeal lipids including those identified in ANME archaea can
367 be found, e.g. those of the abundant Thaumarchaeota (GDGTs with hexose or phosphohexose
368 headgroups, Sinninghe Damsté *et al.*, 2012) and uncharacterized archaea (mainly GDGTs with
369 glycosidic headgroups and in subsurface sediments also archaeol with glycosidic headgroups, Sturt *et*
370 *al.*, 2004; Lipp *et al.*, 2008). In freshwater environments, IPLs of methanotrophic archaea have hardly
371 been studied. Two studies on peat samples identified GDGTs with a glucose or glucuronosyl
372 headgroup (Liu *et al.*, 2010) and with a hexose-glycuronic acid, phosphohexose, or hexose-
373 phosphoglycerol head group (Peterse *et al.*, 2011). GDGTs with a hexose-phosphoglycerol head group
374 were also identified in our study for ANME-2d archaea. Therefore, ANME-2d together with other
375 archaea might be part of the peat microbial community based on the IPL profile. Using DNA
376 biomarkers, most notably the 16S rRNA gene, *Ca. Methanoperedens* sp. has been detected in various
377 peat ecosystems (Cadillo-Quiroz *et al.*, 2008; Zhang *et al.*, 2008; Wang *et al.*, 2019).

378 The related order *Methanosarcinales* mainly produce archaeol and hydroxyarchaeol with the
379 headgroups glucose, phosphatidyl glycerol (only *Methanosarcinaceae*), phosphatidyl inositol,
380 phosphatidyl ethanolamine, galactose (only *Methanosaetaceae*) (Koga *et al.*, 1998). On the other
381 hand, members of the related order *Methanomicrobiales* contain GDGT-0 and archaeol with the lipid
382 headgroups glucose, galactose, phosphatidyl aminopentanetetrols, phosphatidyl glycerol (Koga *et al.*,
383 1998). Therefore, IPLs from *Ca. Methanoperedens* sp. differ from methanogen IPLs by the high
384 abundance of dihexose, MMPE and phosphatidyl hexose as lipid headgroup and the absence of the
385 quite common headgroup phosphatidyl serine.

386

387 **Incorporation of carbon derived from methane and bicarbonate in lipids**

388 We were not only interested in characterizing the lipids of *Ca. Methanoperedens* sp., but also in
389 answering the question if the organism incorporates carbon derived from methane or from dissolved
390 inorganic carbon (DIC) in its lipids. In a labelling experiment from 2006 with an ANME-2d
391 enrichment culture, incorporation of carbon derived from methane could hardly be detected for
392 archaeal lipids (Raghoebarsing *et al.*, 2006). To establish the carbon sources for *Ca. Methanoperedens*
393 sp. we incubated the enrichment culture with ¹³C labelled bicarbonate and methane and analysed lipid
394 extracts for δ¹³C depletion by GC-IRMS (Fig. 2).



395

396 **Figure 2: $\delta^{13}\text{C}$ values of *Ca. Methanoperedens sp.* lipids after batch cultivation with labelled bicarbonate**
397 **or methane.**

398 ANME-2d reactor material originating from the Ooijpolder was incubated in anaerobic batch cultures with either
399 ^{13}C labelled bicarbonate for three days (striped columns) or ^{13}C labelled methane for one (light grey columns) or
400 three days (dark grey columns) and analysed via GC-IRMS. Controls contained only non-labelled carbon sources
401 (white columns). Incubations were performed in triplicates, error bars = standard deviation. Peak identification
402 was conducted with the help of GC-MS analysis of the same samples, showing that lipid extracts contained
403 archaeol, hydroxyarchaeol and two monounsaturated archaeols (Fig. 1). Uns-archaeol = monounsaturated
404 archaeol.

405 Analysis of the isotopic composition of archaeol and its derivatives showed that ANME-2d archaea
406 incorporated carbon derived from both methane and bicarbonate into their lipids. However, the main
407 carbon source for biomass production seemed to be methane and not DIC as the former shows more
408 label in the archaeal lipids. However, it has to be considered that the cultures to which ^{13}C labelled
409 bicarbonate was added did not exclusively contain ^{13}C -DIC. About half of the DIC in the cultures
410 derived from ^{12}C - CO_2 dissolved in the medium after gassing with a mixture of 10% CO_2 /90% Argon
411 gas (calculations in the methods part). Considering this, the $\delta^{13}\text{C}$ values of the archaeol isomers
412 without ^{12}C -DIC in the incubations would vary most probably between -40 and -60‰. Nevertheless,
413 the respective lipids were still quite depleted in $\delta^{13}\text{C}$ in comparison to the incubations with labelled
414 methane (-2 to 12‰; 3 days incubation). Therefore, we concluded that mainly methane and not DIC is
415 incorporated in the lipids of *Ca. Methanoperedens sp.*. Supporting this result, cultures containing
416 marine ANME-1 and ANME-2 were shown to incorporate carbon derived from labelled methane into
417 archaeol, monounsaturated archaeol and biphytanes (Blumenberg *et al.*, 2005). In another study it was
418 found that ANME-1 archaea assimilated primarily inorganic carbon (Kellermann *et al.*, 2012).
419 Incubations with sediments containing ANME-1, 2a & 2b archaea showed that both, labelled methane
420 and inorganic carbon, were incorporated into the archaeal lipids (Wegener *et al.*, 2008). Incubations
421 with freshwater sediments including ANME-2d archaea followed by RNA stable isotope probing
422 demonstrated that those microbes mainly incorporated methane into their lipids but may have the

423 capability of mixed assimilation of CH₄ and dissolved inorganic carbon (Weber *et al.*, 2017). Our data
 424 confirmed that ANME-2d archaea are capable of mixed assimilation of CH₄ and DIC, but that
 425 methane is the preferred carbon source.

426

427 Conclusion

428

429 In this study, we analysed the lipids from the main player in nitrate AOM, *Ca. Methanoperedens* sp.
 430 We found several lipid characteristics that enable distinction between ANME-2d and other ANME
 431 groups (Table 2).

432 Table 2: Lipids of different ANME groups

433 For ANME-2d lipid analysis we used *Ca. Methanoperedens* sp. enriched bioreactor material. For the other
 434 ANME groups information was based on publication about the specific lipid characteristic (Blumenberg *et al.*,
 435 2004; Niemann and Elvert, 2008) or ¹³C labelling experiments (Blumenberg *et al.*, 2005; Wegener *et al.*, 2008;
 436 Kellermann *et al.*, 2012). GDGT: glycerol dialkyl glycerol tetraether, PE: phosphatidyl ethanolamine, MMPE:
 437 monomethyl phosphatidyl ethanolamine, DMPE: dimethyl phosphatidyl ethanolamine, PG: phosphatidyl
 438 glycerol, MH: monohexose, DH: dihexose, PH: phosphatidyl hexose, PC: phosphatidyl choline.

	ANME-1	ANME-2a/b	ANME-2c	ANME-2d	ANME-3
Environment	marine	marine	marine	freshwater	marine
core lipids	GDGT	(OH-) archaeol	(OH-) archaeol, GDGTs	(OH-) archaeol, (OH)-GDGTs	(OH-) archaeol
Sn-2-OH- archaeol / archaeol ratio	0 - 0.8	1.1 - 5.5	1.1 - 5.5	0.1 - 0.3	1.1 - 5.5
IPLs	GDGT + dihexose	(OH-) Archaeol + PG, PE, PH, PS, dihexose	(OH-) Archaeol + PG, PE, PH, PS, Dihexose	(OH-) archaeol + dihexose, hexose, pentose, PH, PE, MMPE, DMPE	(OH-) Archaeol + PG, PH, PS
Main carbon source	DIC			CH₄	

439

440 ANME-2d archaea therefore can be distinguished from ANME-1 by the higher ratio of archaeol and
 441 hydroxyarchaeol instead of GDGTs as well as phosphate containing headgroups. Furthermore,
 442 ANME-2d can be distinguished from other ANME-2 and ANME-3 archaea by the high abundance of
 443 dihexose as headgroup, the rare MMPE and DMPE headgroups and putatively also the pentose
 444 headgroup, which so far has not been described in the literature. The appearance of a monopentose as
 445 headgroup of ANME-2d lipids is an interesting observation and might be further analysed in the
 446 future. In contrast to other ANME groups ANME-2d archaea have been shown to produce relatively
 447 rare hydroxylated GDGTs.

448 ANME groups do not only differ in their membrane lipids itself, but also in the way they incorporate
449 carbon into their biomass. For ANME-1 it has been shown that primarily carbon derived from DIC is
450 incorporated into the lipids (Kellermann *et al.*, 2012). In case of ANME-2d archaea, we were able to
451 demonstrate that both, carbon derived from DIC and from methane, are incorporated into their lipids,
452 with methane as the preferred carbon source.

453

454 Acknowledgements

455 CUW and MSMJ were supported by the Nederlandse Organisatie voor Wetenschappelijk Onderzoek
456 through the Soehngen Institute of Anaerobic Microbiology Gravitation Grant 024.002.002 and the
457 Netherlands Earth System Science Center Gravitation Grant 024.002.001. MSMJ was supported by
458 the European Research Council Advanced Grant Ecology of Anaerobic Methane Oxidizing Microbes
459 339880. JK was supported by the Netherlands Earth System Science Center Gravitation Grant
460 024.002.001 and the Deutsche Forschungs Gesellschaft (DFG) Grant KU 3768/1-1. SB and CW were
461 supported by the Nederlandse Organisatie voor Wetenschappelijk Onderzoek through Grant
462 ALWOP.293. We thank Michel Koenen for IPL analysis, Ronald van Bommel for technical assistance
463 with the GC-IRMS, Denise Dorhout and Monique Verweij for technical assistance with GC-MS and
464 UHPLC systems. Moreover, we thank Annika Vaksmaa for supplying bioreactor material, Theo van
465 Alen for technical assistance with metagenomics sequencing and Jeroen Frank for helping with
466 metagenomics analysis.

467 References

- 468 Arshad, A., Speth, D.R., de Graaf, R.M., Op den Camp, H.J.M., Jetten, M.S.M., and Welte, C.U. (2015)
469 A metagenomics-based metabolic model of nitrate-dependent anaerobic oxidation of methane
470 by *Methanoperedens*-like archaea. *Front. Microbiol.* **6**: 1–14.
- 471 Bale, N.J., Villanueva, L., Hopmans, E.C., Schouten, S., and Sinninghe Damsté, J.S. (2013) Different
472 seasonality of pelagic and benthic Thaumarchaeota in the North Sea. *Biogeosciences* **10**: 7195–
473 7206.
- 474 Beal, E.J., House, C.H., and Orphan, V.J. (2009) Manganese- and iron-dependent marine methane
475 oxidation. *Science*. **325**: 184–187.
- 476 Berger, S., Frank, J., Dalcin Martins, P., Jetten, M.S.M., and Welte, C.U. (2017) High-quality draft
477 genome sequence of “*Candidatus* Methanoperedens sp.” Strain BLZ2, a nitrate-reducing
478 anaerobic methane-oxidizing archaeon enriched in an anoxic bioreactor. *genome Announc.* **5**:
479 e01159-17.
- 480 Blumenberg, M., Seifert, R., Nauhaus, K., and Pape, T. (2005) In vitro study of lipid biosynthesis in an
481 anaerobically methane-oxidizing microbial mat. *Appl. Environ. Microbiol.* **71**: 4345–4351.
- 482 Blumenberg, M., Seifert, R., Reitner, J., Pape, T., and Michaelis, W. (2004) Membrane lipid patterns
483 typify distinct anaerobic methanotrophic consortia. *Proc. Natl. Acad. Sci.* **101**: 11111–11116.
- 484 Boetius, A., Ravensschlag, K., Schubert, C.J., Rickert, D., Widdel, F., Gieseke, A., et al. (2000) A marine
485 microbial consortium apparently mediating anaerobic oxidation of methane. *Nature* **407**: 623–
486 626.
- 487 Cadillo-Quiroz, H., Yashiro, E., Yavitt, J.B., and Zinder, S.H. (2008) Characterization of the archaeal
488 community in a minerotrophic fen and terminal restriction fragment length polymorphism-

- 489 directed isolation of a novel hydrogenotrophic methanogen. *Appl. Environ. Microbiol.* **74**: 2059–
490 2068.
- 491 Cai, C., Leu, A.O., Xie, G.-J., Guo, J., Feng, Y., Zhao, J.-X., et al. (2018) A methanotrophic archaeon
492 couples anaerobic oxidation of methane to Fe (III) reduction. *ISME J.* **12**: 1929–1939.
- 493 Conrad, R. (2009) The global methane cycle: Recent advances in understanding the microbial
494 processes involved. *Environ. Microbiol. Rep.* **1**: 285–292.
- 495 Dean, J.F., Middelburg, J.J., Roeckmann, T., Aerts, R., Blauw, L.G., Egger, M., et al. (2018) Methane
496 feedbacks to the global climate system in a warmer world. *Rev. Geophys.* **56**: 207–250.
- 497 Ekiel, I. and Sprott, G.D. (1992) Identification of degradation artifacts formed upon treatment of
498 hydroxydiether lipids from methanogens with methanolic HCl. *Can. J. Microbiol.* **38**: 764–768.
- 499 Elvert, M., Hopmans, E., Treude, T., Boetius, A., and Suess, E. (2005) Spatial variations of
500 methanotrophic consortia at cold methane seeps: implications from a high-resolution molecular
501 and. *Geobiology* **3**: 195–209.
- 502 Elvert, M., Suess, E., and Whiticar, M.J. (1999) Anaerobic methane oxidation associated with marine
503 gas hydrates: superlight C-isotopes from saturated and unsaturated C₂₀ and C₂₅ irregular
504 isoprenoids. *Naturwissenschaften* **86**: 295–300.
- 505 Ettwig, K.F., Butler, M.K., Le Paslier, D., Pelletier, E., Mangenot, S., Kuypers, M.M.M., et al. (2010)
506 Nitrite-driven anaerobic methane oxidation by oxygenic bacteria. *Nature* **464**: 543–548.
- 507 Ettwig, K.F., Zhu, B., Speth, D., Keltjens, J.T., Jetten, M.S.M., and Kartal, B. (2016) Archaea catalyze
508 iron-dependent anaerobic oxidation of methane. *Proc. Natl. Acad. Sci. U. S. A.* **113**: 127922–
509 12796.
- 510 Franzmann, P.D., Stackebrandt, E., Sanderson, K., Volkman, J.K., Cameron, D.E., Stevenson, P.L., et al.
511 (1988) *Halobacterium lacusprofundi* sp. nov., a halophilic bacterium isolated from Deep Lake,
512 Antarctica. *Syst. Appl. Microbiol.* **11**: 20–27.
- 513 Gibson, J.A.E., Miller, M.R., Davies, N.W., Neill, G.P., Nichols, D.S., and Volkman, J.K. (2005)
514 Unsaturated diether lipids in the psychrotrophic archaeon *Halorubrum lacusprofundi*. *Syst.*
515 *Appl. Microbiol.* **28**: 19–26.
- 516 Hafenbradl, D., Keller, M., Thiericke, R., and Stetter, K.O. (1993) A novel unsaturated archaeal ether
517 core lipid from the hyperthermophile *Methanopyrus kandleri*. *Syst. Appl. Microbiol.* **16**: 165–
518 169.
- 519 Hallam, S.J., Putnam, N., Preston, C.M., Detter, J.C., Rokhsar, D., Richardson, P.M., and DeLong, E.F.
520 (2004) Reverse methanogenesis: testing the hypothesis with environmental genomics. *Science*.
521 **305**: 1457–1463.
- 522 Haroon, M.F., Hu, S., Shi, Y., Imelfort, M., Keller, J., Hugenholtz, P., et al. (2013) Anaerobic oxidation
523 of methane coupled to nitrate reduction in a novel archaeal lineage. *Nature* **500**: 567–570.
- 524 Hinrichs, K.-U., Hayes, J.M., Sylva, S.P., Brewer, G.B., and DeLong, E.F. (1999) Methane-consuming
525 archaeobacteria in marine sediments. *Nature* **398**: 802–805.
- 526 Hinrichs, K.-U., Pancost, R.D., Summons, R.E., Sprott, G.D., Sylva, S.P., Sinninghe Damsté, J.S., and
527 Hayes, J.M. (2000) Mass spectra of sn-2-hydroxyarchaeol, a polar lipid biomarker for anaerobic
528 methanotrophy. *Geochemistry Geophys. Geosystems* **1**: 2000GC000042.
- 529 Hinrichs, K. and Boetius, A. (2002) The anaerobic oxidation of methane: new insights in microbial
530 ecology and biogeochemistry. In: Wefer, G., Billett, D., Hebbeln, D., Jørgensen, B., Schlüter, M.,
531 and van Weering, T. (eds), *Ocean margin systems*. Springer-Verlag, Berlin, pp. 457–477.

- 532 Hoehler, T.M., Alperin, M.J., Albert, D.B., and Martens, C.S. (1994) Field and laboratory studies of
533 methane oxidation in an anoxic marine sediment: Evidence for a methanogen-sulfate reducer
534 consortium. *Global Biogeochem. Cycles* **8**: 451–463.
- 535 Hu, S., Zeng, R.J., Burow, L.C., Lant, P., Keller, J., and Yuan, Z. (2009) Enrichment of denitrifying
536 anaerobic methane oxidizing microorganisms. *Environ. Microbiol. Rep.* **1**: 377–384.
- 537 Kellermann, M.Y., Wegener, G., Elvert, M., Yoshinaga, M.Y., Lin, Y.-S., Holler, T., et al. (2012)
538 Autotrophy as a predominant mode of carbon fixation in anaerobic methane-oxidizing microbial
539 communities. *Proc. Natl. Acad. Sci.* **109**: 19321–19326.
- 540 Knittel, K. and Boetius, A. (2009) Anaerobic oxidation of methane: progress with an unknown
541 process. *Annu. Rev. Microbiol.* **63**: 311–334.
- 542 Koga, Y. and Morii, H. (2007) Biosynthesis of ether-type polar lipids in Archaea and evolutionary
543 considerations. *Microbiol. Mol. Biol. Rev.* **71**: 97–120.
- 544 Koga, Y., Morii, H., Akagawa-Matsushita, M., and Ohga, M. (1998) Correlation of polar lipid
545 composition with 16S rRNA phylogeny in methanogens. Further analysis of lipid component
546 parts. *Biosci. Biotechnol. Biochem.* **62**: 230–236.
- 547 Koga, Y., Nishihara, M., Morii, H., and Akagawa-Matsushita, M. (1993) Ether polar lipids of
548 methanogenic bacteria: structures, comparative aspects, and biosyntheses. *Microbiol. Rev.* **57**:
549 164–182.
- 550 Kool, D.M., Zhu, B., Rijpstra, W.I.C., Jetten, M.S.M., Ettwig, K.F., and Sinninghe Damsté, J.S. (2012)
551 Rare branched fatty acids characterize the lipid composition of the intra-aerobic methane
552 oxidizer “*Candidatus Methylopirabilis oxyfera*.” *Appl. Environ. Microbiol.* **78**: 8650–8656.
- 553 Lipp, J.S., Morono, Y., Inagaki, F., and Hinrichs, K.-U. (2008) Significant contribution of Archaea to
554 extant biomass in marine subsurface sediments. *Nat. Lett.* **454**: 991–994.
- 555 Liu, X.-L., Lipp, J.S., Simpson, J.H., Lin, Y.-S., Summons, R.E., and Hinrichs, K.-U. (2012) Mono- and
556 dihydroxyl glycerol dibiphytanyl glycerol tetraethers in marine sediments: Identification of both
557 core and intact polar lipid forms. *Geochim. Cosmochim. Acta* **89**: 102–115.
- 558 Liu, X., Leider, A., Gillespie, A., Gröger, J., Versteegh, G.J.M., and Hinrichs, K.-U. (2010) Organic
559 Geochemistry Identification of polar lipid precursors of the ubiquitous branched GDGT orphan
560 lipids in a peat bog in Northern Germany. *Org. Geochem.* **41**: 653–660.
- 561 Matsumi, R., Atomi, H., Driessen, A.J.M., and van der Oost, J. (2011) Isoprenoid biosynthesis in
562 archaea - biochemical and evolutionary implications. *Res. Microbiol.* **162**: 39–52.
- 563 McAnulty, M.J., Poosarla, V.G., Kim, K.-Y., Jasso-Chávez, R., Logan, B.E., and Wood, T.K. (2017)
564 Electricity from methane by reversing methanogenesis. *Nat. Commun.* **8**: 15419.
- 565 Menzel, P., Ng, K.L., and Krogh, A. (2016) Fast and sensitive taxonomic classification for
566 metagenomics with Kaiju. *Nat. Commun.* **7**: 1–9.
- 567 Nauhaus, K., Albrecht, M., Elvert, M., Boetius, A., and Widdel, F. (2007) In vitro cell growth of marine
568 archaeal-bacterial consortia during anaerobic oxidation of methane with sulfate. *Environ.*
569 *Microbiol.* **9**: 187–196.
- 570 NCBI Resource Coordinators (2016) Database resources of the National Center for Biotechnology
571 Information. *Nucleic Acids Res.* **44**: 7–19.
- 572 Nichols, P.D. and Franzmann, P.D. (1992) Unsaturated diether phospholipids in the Antarctic
573 methanogen *Methanococcoides burtonii*. *FEMS Microbiol. Lett.* **98**: 205–208.
- 574 Nichols, P.D., Shaw, P.M., Mancuso, C.A., and Franzmann, P.D. (1993) Analysis of archaeal

- 575 phospholipid-derived di- and tetraether lipids by high temperature capillary gas
576 chromatography. *J. Microbiol. Methods* **18**: 1–9.
- 577 Niemann, H. and Elvert, M. (2008) Diagnostic lipid biomarker and stable carbon isotope signatures of
578 microbial communities mediating the anaerobic oxidation of methane with sulphate. *Org.*
579 *Geochem.* **39**: 1668–1677.
- 580 Niemann, H., Lösekann, T., de Beer, D., Elvert, M., Nadalig, T., Knittel, K., et al. (2006) Novel microbial
581 communities of the Haakon Mosby mud volcano and their role as a methane sink. *Nature* **443**:
582 854–858.
- 583 Nishihara, M., Morii, H., Matsuno, K., Ohga, M., Stetter, O., and Koga, Y. (2002) Structural analysis by
584 reductive cleavage with LiAlH₄ of an allyl ether choline-phospholipid, archaetidylcholine, from
585 the hyperthermophilic methanoarchaeon *Methanopyrus kandleri*. *Archaea* **1**: 123–131.
- 586 Orphan, V.J., House, C.H., Hinrichs, K.-U., McKeegan, K.D., and DeLong, E.F. (2002) Multiple archaeal
587 groups mediate methane oxidation in anoxic cold seep sediments. *Proc. Natl. Acad. Sci. U. S. A.*
588 **99**: 7663–7668.
- 589 Pancost, R.D., Hopmans, E.C., and Sinninghe Damsté, J.S. (2001) Archaeal lipids in mediterranean cold
590 seeps: molecular proxies for anaerobic methane oxidation. *Geochim. Cosmochim. Acta* **65**:
591 1611–1627.
- 592 Pancost, R.D., Sinninghe Damsté, J.S., de Lint, S., van der Maarel, M.J.E.C., and Gottschal, J.C. (2000)
593 Biomarker evidence for widespread anaerobic methane oxidation in mediterranean sediments
594 by a consortium of methaogenic archaea and bacteria. *Appl. Environ. Microbiol.* **66**: 1126–1132.
- 595 Peterse, F., Hopmans, E.C., Schouten, S., Mets, A., Rijpstra, W.I.C., and Sinninghe Damsté, J.S. (2011)
596 Identification and distribution of intact polar branched tetraether lipids in peat and soil. *Org.*
597 *Geochem.* **42**: 1007–1015.
- 598 Raghoebarsing, A.A., Pol, A., van de Pas-Schoonen, K.T., Smolders, A.J.P., Ettwig, K.F., Rijpstra, W.I.C.,
599 et al. (2006) A microbial consortium couples anaerobic methane oxidation to denitrification.
600 *Nature* **440**: 918–921.
- 601 De Rosa, M. and Gambacorta, A. (1988) The lipids of archaeobacteria. *Prog. Lipid Res.* **27**: 153–175.
- 602 Rossel, P.E., Lipp, J.S., Fredricks, H.F., Arnds, J., Boetius, A., Elvert, M., and Hinrichs, K.U. (2008) Intact
603 polar lipids of anaerobic methanotrophic archaea and associated bacteria. *Org. Geochem.* **39**:
604 992–999.
- 605 Ruetters, H., Sass, H., Cypionka, H., and Rullkoetter, J. (2002) Phospholipid analysis as a tool to study
606 complex microbial communities in marine sediments. *J. Microbiol. Methods* **48**: 149–160.
- 607 Schouten, S., Hopmans, E.C., and Sinninghe Damsté, J.S. (2012) The organic geochemistry of glycerol
608 dialkyl glycerol tetraether lipids: A review. *Org. Geochem.* **54**: 19–61.
- 609 Sinninghe Damsté, J.S., Rijpstra, W.I.C., Hopmans, E.C., Jung, M.-Y., Kim, J.-G., Rhee, S.-K., et al.
610 (2012) Intact polar and core glycerol dibiphytanyl glycerol tetraether lipids of group I.1a and
611 I.1b Thaumarchaeota in soil. *Appl. Environ. Microbiol.* **78**: 6866–6874.
- 612 Sturt, H.F., Summons, R.E., Smith, K., Elvert, M., and Hinrichs, K. (2004) Intact polar membrane lipids
613 in prokaryotes and sediments deciphered by high-performance liquid chromatography /
614 electrospray ionization multistage mass spectrometry — new biomarkers for biogeochemistry
615 and microbial ecology. 617–628.
- 616 Timmers, P.H.A., Welte, C.U., Koehorst, J.J., Plugge, C.M., Jetten, M.S.M., and Stams, A.J.M. (2017)
617 Reverse methanogenesis and respiration in methanotrophic archaea. *Archaea* **2017**: 1654237.
- 618 Vaksmaa, A., Guerrero-Cruz, S., van Alen, T.A., Cremers, G., Ettwig, K.F., Lüke, C., and Jetten, M.S.M.

- 619 (2017) Enrichment of anaerobic nitrate-dependent methanotrophic “*Candidatus*
620 *Methanoperedens nitroreducens*” archaea from an Italian paddy field soil. *Appl. Microbiol.*
621 *Biotechnol.* **101**: 7075–7084.
- 622 Vaksmaa, A., Jetten, M.S.M., Ettwig, K.F., and Lücke, C. (2017) *McrA* primers for the detection and
623 quantification of the anaerobic archaeal methanotroph “*Candidatus* *Methanoperedens*
624 *nitroreducens*.” *Appl. Microbiol. Biotechnol.* **101**: 1631–1641.
- 625 Wang, M., Tian, J., Bu, Z., Lamit, L.J., Chen, H., Zhu, Q., and Peng, C. (2019) Structural and functional
626 differentiation of the microbial community in the surface and subsurface peat of two
627 minerotrophic fens in China. *Plant Soil.* doi.org/10.1007/s11104-019-03962-w.
- 628 Weber, H.S., Habicht, K.S., and Thamdrup, B. (2017) Anaerobic methanotrophic archaea of the
629 ANME-2d cluster are active in a low-sulfate, iron-rich freshwater sediment. *Front. Microbiol.* **8**:
630 1–13.
- 631 Wegener, G., Niemann, H., Elvert, M., Hinrichs, K.U., and Boetius, A. (2008) Assimilation of methane
632 and inorganic carbon by microbial communities mediating the anaerobic oxidation of methane.
633 *Environ. Microbiol.* **10**: 2287–2298.
- 634 Zhang, G., Tian, J., Jiang, N., Guo, X., Wang, Y., and Dong, X. (2008) Methanogen community in Zoige
635 wetland of Tibetan plateau and phenotypic characterization of a dominant uncultured
636 methanogen cluster ZC-I. *Environ. Microbiol.* **10**: 1850–1860.
- 637